Journal of Microscopy, Vol. 174, Pt 2, May 1994, pp. 101–110.
Received 8 February 1993; accepted 18 January 1994

Method for the study of the three-dimensional orientation of the nuclei of myocardial cells in fetal human heart by means of confocal scanning laser microscopy

Y. USSON,* F. PARAZZA,* P.-S. JOUK*† & G. MICHALOWICZ†
**Dynamique de l'organisation du génome, Université Joseph Fourier, BP53, 38041 Grenoble cedex 9, France*
†*Médecine Néonatale, Centre Hospitalier Régional Universitaire, Grenoble, France*

Key words. Confocal scanning laser microscopy, three-dimensional image analysis, three-dimensional feature extraction, normal fetal heart, cardiomyopathies.

Summary

A series of three-dimensional image analysis tools are used to measure the three-dimensional orientation of nuclei of myocardial cells. Confocal scanning laser microscopy makes it possible to acquire series of sections up to 100 μm inside thick tissue sections. A mean orientation vector of unit length is calculated for each segmented nucleus. The global orientation statistics are obtained by calculating the vectorial sum of the nuclear unit vectors. The final orientation is expressed by a mean azimuth angle, an elevation angle and a measure of the angular homogeneity. The method is illustrated for two different regions of the myocardium (interventricular septum and papillary muscle) of a normal human fetal heart. This quantitative method will be used to assess and calibrate the information provided by polarized light microscopy.

Introduction

The topographical organization of cardiac myofibres in fetal heart depends on two factors: the migration of the embryonic cardiac compounds during morphogenesis and mechanical stress developed in fetal ventricular walls. The knowledge of that organization is a basic requirement for the understanding of fetal and neonatal myocardiopathies.

The adult ventricular myocardium is a muscle made of a three-dimensional (3-D) network of myocardial cells connected by anastomoses. This network or connection pattern is highly structured and was described as a multilayered organization where each layer of myocardial cells has a preferred orientation (Streeter, 1979). This pattern has been studied with three different approaches: mechanical peeling of the heart from epicardium to endocardium (Torrent-Guasp, 1973); study of macroscopical serial sections (Hort, 1960); and histological study of sampled regions (Streeter & Hanna, 1973). The studies of the myocardial histogenesis mainly addressed myofibrillogenesis (Manasek, 1970), the rate of cellular proliferation and the capacity of hypertrophy (Zak, 1984).

Different methods to investigate the organization of myocardial fibres in the normal heart and in cardiomyopathies have been developed at the macroscopic and microscopic levels. These were based mainly on semi-automatic quantitative techniques (Maron & Roberts, 1979; McLean & Prothero, 1987, 1991), where an operator draws on a digitizer tablet the main axis of the in-plane fibres. A different and more sophisticated technique was used by Whittaker *et al.* (1989). The thin sections were observed by polarized light microscopy. Muscles cells were selected on a stereological grid, then the stage of the microscope was rotated until the cells were at extinction. The extinction angle was recorded as the cell orientation angle. Although these techniques provide information about the azimuth angle, they lack information about the obliquity of fibres (i.e. the elevation angle).

In this paper we present an original approach to characterize the orientation of myocardial cells in normal fetal heart. Developmental studies based on muscle fibre teasing techniques showed that the nuclei of the skeletal muscular cells are elongated ovoids distributed almost regularly along the fibres 'like a pearl necklace' (Harris *et al.*, 1989). Ultrastructural 3-D reconstruction of normal developing skeletal muscular cells showed a strong correlation between the main orientation of the nuclei and the orientation of the reconstructed fibres (Duxson *et al.*, 1989). The shape of myocardial cell nuclei was also described using light microscopy at various stages of

development of the human heart (Adler *et al.*, 1977). The particular shape of the nuclei and their regular distribution along the fibre can be exploited. Thus, the nuclei can be considered as good clues to the myocardial cell orientation. However, the analysis of the shape and orientation of the nuclei on thin tissue sections would only give information on the azimuth angle. Therefore it is necessary to undertake such a study at a 3-D level. The confocal scanning laser microscope (CSLM) is a powerful tool for investigating tissues in three dimensions (Carlsson & Aslund, 1987). A recent paper by Clarke *et al.* (1993) demonstrated the efficiency of CSLM for measuring the orientation of fibre structures. In recent years a number of developments in 3-D image analysis have made it possible to undertake quantitative morphological studies of nuclei (Rigaut *et al.*, 1990; Rigaut & Vassy, 1991; Kett *et al.*, 1992; Humbert *et al.*, 1992; Parazza *et al.*, 1993). We developed a method to measure from CSLM data sets the orientations of myocardial cell nuclei in normal fetal human heart. These orientations were expressed in polar coordinates, i.e. for each nucleus an azimuth angle (projection angles on the section plane) and an elevation angle (obliquity angles with reference to the section plane) were calculated. This method is used to assess the measurement of orientations of myocardial cells in polarized light (Jouk *et al.*, 1994).

Materials and methods

Human fetal hearts

Human fetal hearts (at 14–40 weeks gestation) were fixed by perfusion with 4% neutral buffered formalin. They were then bathed for 1 week in the same solution.

Histological preparation

Embedding. The hearts were embedded in a resin of methyl methacrylate (MMA) using the following protocol. The specimens were infiltrated at room temperature with two solutions of glycol methacrylate (GMA) in water of increasing concentration (each for 1 week), followed by immersion in pure GMA for 1 week. They were then infiltrated for 1 week in a series of mixtures of GMA and MMA in which the concentration of MMA was gradually increased to 100%. The hearts were embedded by polymerization of MMA at 305 K.

Fiducials. In order to have a constant anatomical reference for further orientation analysis, the hearts were held vertical during the polymerization process. This was achieved by transfixing with a thin needle through the interventricular septum along a baso-apical axis of the heart. After polymerization, four holes (block fiducials, diameter 1 mm) were drilled in the embedding resin at constantly registered positions with their axes parallel to the baso-apical axis of the heart. The reference system for the 3-D space was defined as follows: the xy-plane corresponds to the section plane with the y-axis parallel to the interventricular septum; the z-axis is aligned with the baso-apical axis of the heart.

Sectioning. For every heart, a series of thick sections (500 μm) was cut with a rotary microtome (1600, Leica). The rate of penetration of the rotary saw was set at a low speed (15 min per section) in order to avoid mechanical stress and distortions.

Staining. After examination by polarized light microscopy, some selected sections were stained with Feulgen for confocal scanning laser microscopy. The sections were stained prior to mounting them on glass slides. In this way the solutions could penetrate the thick sections on both sides which ensures in-depth staining. Because the sections were not deplastified they were highly hydrophobic and it was necessary to permeabilize these with a solution of 20% tetrahydrofurane (THF) in water. After hydrolysis in 6 N HCl for 2 h at room temperature, the sections were rinsed in water and left in Schiff reagent for 4 h at room temperature. They were then left in four baths of bisulphite water 0·5% for 10 min each, and rinsed in water. After coloration, the sections were laid on glass slides in a 20% solution of THF to help them spread. After 2 h the slides were rinsed in water, and mounted with an anti-fading solution under coverslips.

Microscopy

Polarized light microscopy. The thick sections were analysed with an SV11 stereomicroscope (Zeiss) equipped for polarized light (Whittaker *et al.*, 1989). Two images per section were recorded with a CCD video camera and digitized for two different angles (0° and 45°) of the specimen with reference to the polarizer. After registration of the grey levels (*i.e.* light intensities) of the two digitized images these were combined using a digital maximum operator. This resulted in a segmentation of organized co-planar myofibres versus either disorganized or oblique fibres. The grey level information of the combined images could be interpreted as a function of the elevation and azimuth angles of the fibre bundles.

Confocal scanning laser microscopy. Selected zones of the Feulgen-stained slides were investigated with a confocal scanning laser microscope LSM10 (Zeiss, Oberkochen, Germany). Fluorescence of the Feulgen dye was obtained using a helium–neon laser with an excitation wavelength of 543 nm. Emitted light was collected through an oil-

immersion objective lens (40×, NA 1·3, Planapo Neofluar, Zeiss), and transmitted to the photomultiplier through a long-pass filter with a cut-off wavelength of 590 nm. At this setting the resolutions measured with fluorescent microbeads were 0·25 μm in the xy-plane and 0·94 μm along the z-axis. In order to collect cubic data, the voxels were sampled every 0·47 μm in the in-focus plane and the microscope stage was raised by 0·47 μm between the recording of each optical section. Every optical section was recorded eight times for image averaging with a scanning time of 1·8 s per field. The sections were stored as a series of 200 digital images (256 × 256 pixels) corresponding to a final volume of 120 × 120 μm × 95 μm representing a final amount of 13 Mbytes of data.

Three-dimensional image analysis

The 3-D analysis and reconstruction programs were written in C language on an Iris Indigo Entry (Silicon Graphics, Mountain View, U.S.A.) fitted with 32 Mbytes of memory. Some of the algorithms have been already described (Parazza *et al.*, 1993).

Preprocessing. A series of processing steps were applied to the 3-D voxel set in order to facilitate the segmentation of nuclei. First, it was necessary to compensate for the attenuation of fluorescence emission intensity as a function of depth in the tissue as well as for photobleaching. The intensity levels were corrected in every section using a log-logistic equation (Rigaut *et al.*, 1990; Rigaut & Vassy, 1991). Secondly a 3-D median operator (3 × 3 × 3 Kernel) was used to filter out pulse noise from the voxel volume. Thereafter, a 3-D grey-level morphological opening was applied in order to increase the separability of the nuclei. The kernel for filtering was based on 3 × 3 × 3 cube without the corner voxels (van der Voort *et al.*, 1989).

Segmentation. Segmentation of the nuclei was achieved by a simple grey level thresholding. The value of the threshold was set after examining the 3-D grey-level histogram. However, some nuclei could not be separated using this threshold. In such cases an interactive 3-D editing utility was used to define segmentation planes between touching nuclei. Three orthogonal views (xy, xz and yz) of the unsegmented nuclei were displayed. The user could then draw lines onto the three views that define a 3-D planar surface to be used for separating touching nuclei. At the end of the segmentation process the connected components corresponding to each separate nucleus were labelled using the seed-fill algorithm described in Parazza *et al.* (1993).

Feature extraction. Calculation of the mean orientation of a nucleus was based on fitting a tri-axial ellipsoid to the shape of the nucleus. A similar technique was used by Kett *et al.* (1992) to localize structures in a nucleus. The shape of a nucleus was characterized by the spatial distribution of its surface voxels. The definition of a surface voxel is given by Eq. (1) (see mathematical appendix). In practice, a nuclear voxel was considered to pertain to the nuclear surface if at least one of its 26 direct neighbours did not belong to the nucleus. Every surface voxel was considered to be a single 3-D point whose coordinates were translated such that the origin of the coordinate space coincided with the centre of gravity of the nucleus (Eqs. 2 and 3). The orientation of the fitted ellipsoid was obtained by diagonalization of the matrix of the inner products of the coordinate vectors (Eqs. 4 and 5). The latent roots gave the half-axes of the ellipsoid. The latter were used to filter out contaminating red blood cells. When the ratio of the second axis versus the first axis was greater than 0·80 and the ratio of the third axis versus the second axis was smaller than 0·25, the structure detected was considered to be a red blood cell and was therefore rejected. Finally, the orientation of a nucleus was expressed by means of a vector with unit length, as defined by Eq. (6). This 3-D vector can be expressed as a function of azimuth angle (longitude) and elevation angle (latitude, Eq. 7; Batschelet, 1981). The statistical information for a block of tissue was obtained by calculating a mean azimuth angle ϕ corresponding to the mean orientation of the projections of the nuclear orientations on the section plane, and a mean elevation angle θ corresponding to the obliquity of nuclear orientations with reference to the section plane (Eq. 8; Batschelet, 1981). The homogeneity of the nuclear orientation is given by Eq. (9) (Appendix). To obtain complete information about the distribution of the nuclear orientation we used another measurement of anisotropy based on the values of the latent roots of the matrix of direction cosines (Eq. 10), introduced by Anderson & Stephens (1972), which was applied by other authors to the characterization of the directional distribution of spatial fibre processes using CSLM (Mattfeldt *et al.*, 1994).

Three-dimensional visualization. Three-dimensional reconstruction was used in order to control the results of the segmentation of nuclei. Image synthesis techniques based on a simple shading model (Newman & Sproull, 1981) were used to visualize the surface of the segmented nuclei. The nuclear orientation vectors were displayed with a home-made 3-D software package.

Results

Polarized light microscopy

Figure 1 illustrates the use of polarized light to investigate fibre organization. The light intensity collected is a function of the elevation angle of the fibre bundles and also of their

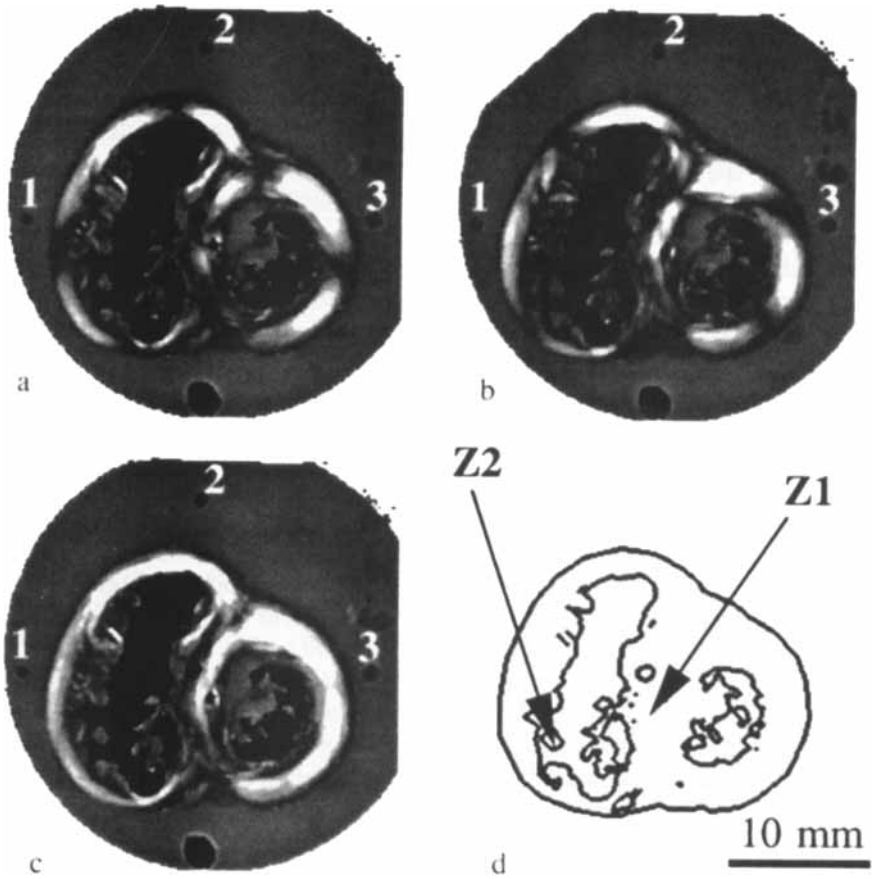

Fig. 1. Polarized light analysis of a thick section of a human fetal heart. The intensity of light is dependent on the three-dimensional orientation of the myocardial fibres. (a) Polarization axis parallel to the interventricular septum. (b) Polarization axis rotated 45° anticlockwise. (c) Combination of images (a) and (b) by a maximum operator. (d) Location of regions selected for confocal scanning laser microscopical analysis: Z1, interventricular septum region; Z2, pillar region. 1, 2 and 3, block fiducials.

azimuth angle. For this reason it is necessary to record at least two images at different angles with reference to the vibration axis of the polarizer. Figure 1(a,b) show the images obtained for angles of 0° and 45°, respectively. When comparing these two images it can be seen that there are different types of response to the rotation of the polarization axis. Some regions of the cardiac muscle are dark in Fig. 1(a, b). This means that these fibres are almost orthogonal to the section plane. Regions that are bright in Fig. 1(a) and dark in Fig. 1(b) correspond to fibres running in parallel with the section plane and whose azimuth angle ranges from 22·5 to 67·5° (modulo 90°) with reference to the polarization axis. Regions that are dark in Fig. 1(a) and bright in Fig. 1(b) correspond to fibres running in parallel with the section plane but whose azimuth angle ranges from −22·5 to 22·5° (modulo 90°). The result of the combination of these two images with a maximum operator is an image (Fig. 1c) in which the light intensity can be interpreted in terms of elevation angle and is altered very little by the azimuth angles information (Jouk *et al.*, 1994). Figure 1(c) shows the two regions that were selected for the 3-D image analysis. Z1 corresponds to a region of the interventricular septum; the bright intensity of that spot in both Fig. 1(b) and Fig. 1(c) means that the fibres are expected to run nearly in parallel to the section plane and with an azimuth angle nearly parallel to the orientation of the interventricular septum. Z2 corresponds to a papillar muscle in a heart pillar; its low intensity in all images indicates that the fibres are orthogonal to the section plane.

Confocal scanning laser microscopy

The acquisition and storage of each 256 × 256 × 200 voxel volume took 50 min. The preprocessing (noise filtering and intensity loss compensation), thresholding and labelling process took 10 min. The interactive separation of touching nuclei took between 15 and 90 min depending on the degree of compactness of the nuclei in the data set. The extraction of nuclear surface voxels and the computation of the nuclear orientations took 15 min. Therefore, the amount of time necessary to obtain the orientation information of selected zones ranged from 1 h 30 min to 2 h 45 min.

Figure 2 shows the 3-D reconstructions of the segmented nuclei for the interventricular region (Fig. 2a) and the pillar region (Fig. 2b). The viewing angle of the reconstruction was selected in order to highlight the degree of organization of the nuclei. The septum region (Fig. 2b) shows a very high level of organization; the nuclear major axes are mainly orientated orthogonal to the section plane, as may be

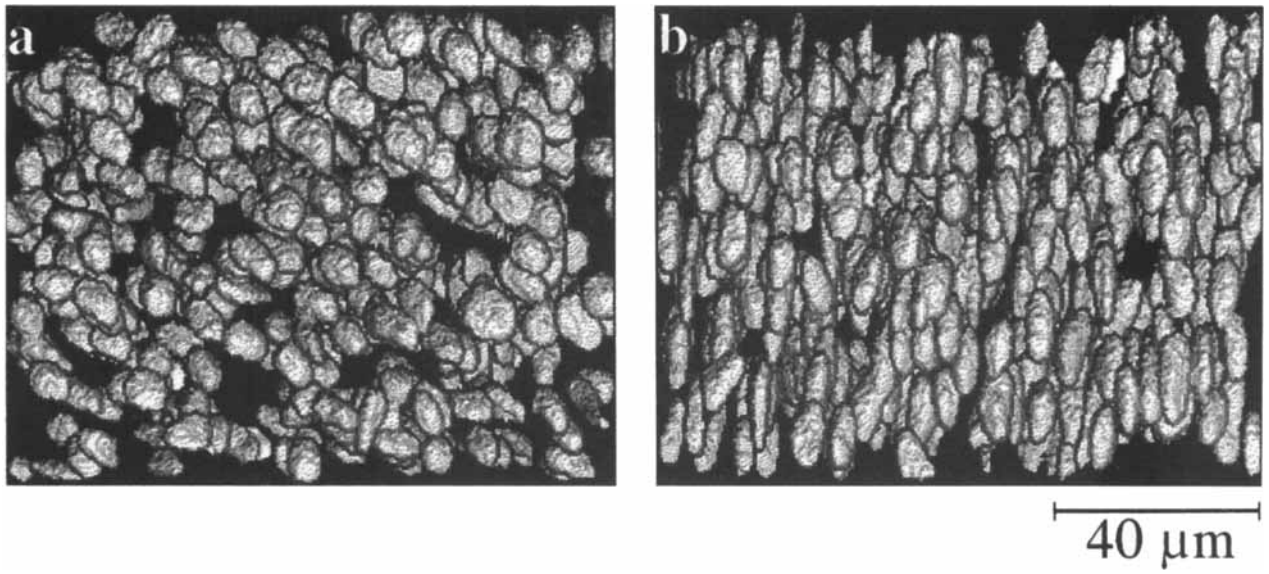

Fig. 2. Segmentation of the three-dimensional data sets. (a) Reconstructed view of the interventricular septum data. (b) Reconstructed view of the pillar data. The angle of view is the same for the two reconstructions and is pointing to the *yz*-plane, i.e. the projection plane of the reconstructed views is orthogonal to the section plane and is orthogonal to the interventricular septum axis.

expected from the polarized light qualitative analysis. The interventricular septum also shows a high level of organization, but to a lower extent than the septum region. In particular, there is a greater heterogeneity in the elevation angles. The major axes of the nuclei are slightly tilted with reference to the section plane.

Analysis of three-dimensional nuclear orientations

The 3-D nuclear orientations were calculated after extraction of the nuclear surface voxels. For each nucleus the major orientation was expressed as a vector of unit length. These vectors were plotted in block diagrams (Fig. 3, top row). This representation stresses the degree of organization of the nuclear orientations and we may easily extrapolate the nuclear orientations by mentally joining the unit vectors to form virtual fibres.

Statistical analysis of the distribution unit vectors allowed us to extract the mean azimuth and elevation angles for the two regions studied (Table 1). The distributions were summarized using polar diagrams (Fig. 3).

Interventricular septum region. A number of nuclei (316) were obtained after segmentation of the 3-D data set. The distribution of the azimuth angle (Fig. 3, left column, middle row) shows there are two main orientation lobes. One lobe is centred on $-90°$ and the other lobe on $50°$. This indicates that the regions contain two main fibre bundles that are interpenetrating. One runs in parallel with the axis of the interventricular septum, and the second represents fibres that originate from the wall of the right ventricule. The distribution of the elevation angle (Fig. 3, left column, bottom row) shows one major lobe centred on $45°$. Thus, most of the nuclei are tilted with reference to the section plane. The presence of these two bundles is indicated by the low value for the angular homogeneity (36.8%, Table 1). However, it can be seen that the values of the latent roots are very different from each other, with $\tau 3$ significantly greater than $\tau 2$ and $\tau 1$ (Table 1). This indicates a strong anisotropy and may seem to contradict the value of angular homogeneity.

Pillar region. A number of nuclei (329) were obtained after segmentation of the 3-D data set. The distribution of the azimuth angle (Fig. 3, right column, middle row) shows a major lobe centred on $40°$ but spread over a large range of angles ($-85°$ to $0°$). In contrast, the histogram of the elevation angle (Fig. 3, right column, bottom row) shows a very narrow lobe centred on $90°$. Indeed, this points out the very high level of organization of the fibre bundles in the pillar, as expressed by the 3-D angular homogeneity (96·7%, Table 1). This homogeneity is in agreement with the measure of the anisotropy. The fibres run in parallel to the baso-apical axis of the heart. Also, the very narrow distribution of the elevation angle explains the heterogeneity of the azimuth angles. The projections of the unit vectors on the section plane are either dimensionless points (elevation of $90°$) or are vectors with a modulus smaller than the magnitude of the segmentation noise. Therefore, in this case the value of the azimuth angle is undefined.

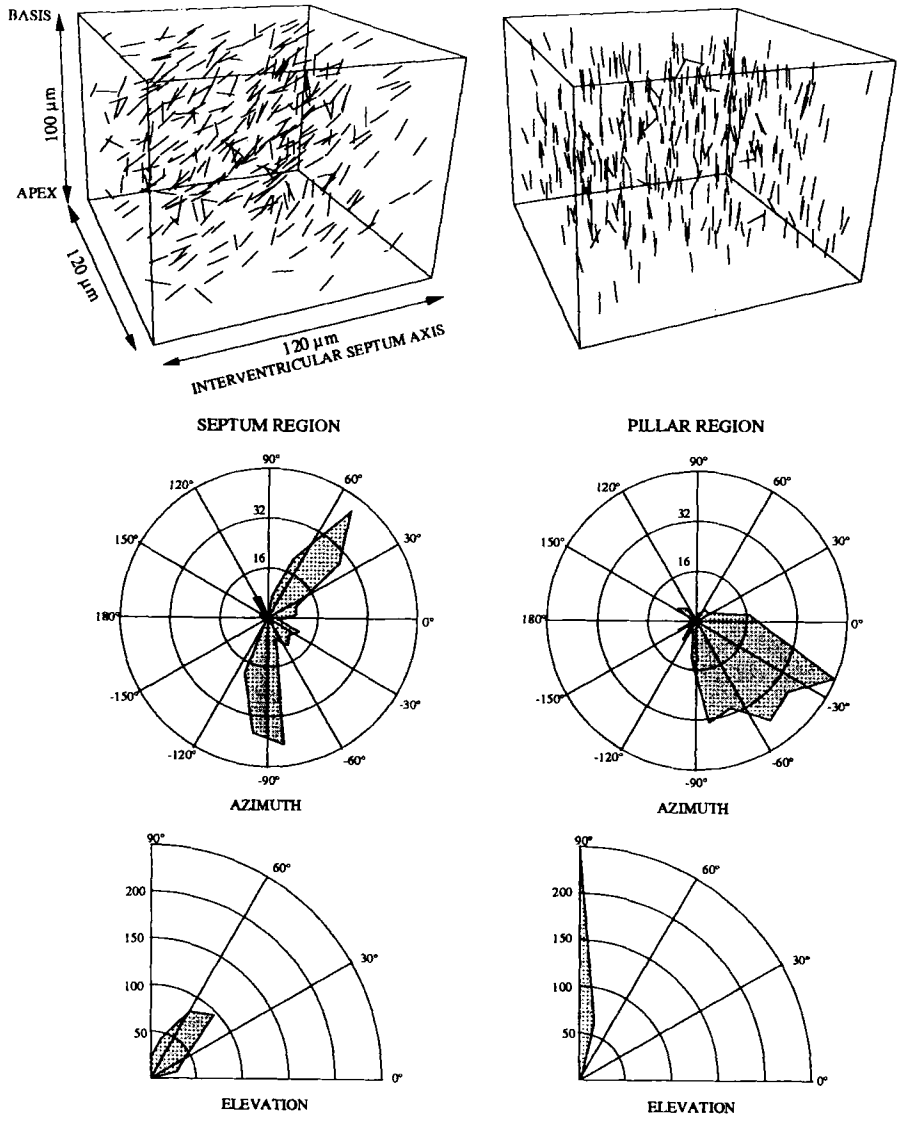

Fig. 3. Three-dimensional analysis of the orientation of the nuclei of myocardial cells. Left column: interventricular septum region. Right column: pillar region. Top row: 3-D block diagrams of the nuclear unit vectors (for the sake of readability the unit vectors are scaled to a length of 10 μm). The block dimensions are 120 μm (width) by 120 μm (depth) by 100 μm (height). Middle row: orientation histograms of the azimuth angle (projection angles on the section plane). The reference of the diagrams is set such that the $-90°$ to $90°$ direction is parallel to the interventricular septum axis. The concentric circles correspond to 16, 32 and 48 nuclei, respectively. Bottom row: orientation histograms of the elevation angle (obliquity angles with reference to the section plane). 0° elevation angle: parallel to the section plane; 90°: parallel to the baso-apical axis of the heart. The concentric circular arcs correspond to 50, 100, 150, 200 and 250 nuclei, respectively.

Discussion

Confocal laser scanning microscopy is a powerful tool for imaging the organization of myocardial fibres. It is possible to investigate the shape and distribution of fluorescent nuclei inside thick sections. It is necessary to associate this technique of microscopy with sophisticated methods of 3-D image analysis and 3-D feature extraction to obtain quantitative information. However, the significance of the orientation measurements is dependent on the accuracy of the segmentation procedure.

Segmentation

A very simple segmentation scheme was used. Selection of the grey-level threshold remained subjective and was

Table 1. Three-dimensional nuclear orientation analysis.

	Homogeneity (%)	ϕ azimuth	θ elevation	Latent roots
Septum	36·8	−47·8°	43·7°	0·80, 0·12, 0·08
Pillar	96·7	−46·2°	82·1°	0·55, 0·28, 0·17

The angular homogeneity is expressed in per cent ($H \times 100$, see Appendix, Eq. 9). The anisotropy is expressed by the relative importance of the eigenvalues of the matrix of the direction cosines (Appendix, Eq. 10): $\tau 3/\tau$, $\tau 2/\tau$, $\tau 1/\tau$ where $\tau 3 \geqslant \tau 2 \geqslant \tau 1$ and $\tau = \tau 1 + \tau 2 + \tau 3$.

chosen in order to reduce as far as possible the number of clusters of touching nuclei while preserving the nuclear shapes and sizes. A morphological grey opening filter was used to improve the resolution of nuclei. Thereafter, the touching nuclei were separated interactively with a 3-D editing tool. Another approach, less time consuming, would be to eliminate the clusters of touching nuclei using a simple size criterion. The attenuation of fluorescence emission intensity as a function of depth could be another source of error. Correction of this attenuation by a log–logistic function equalized the average fluorescence intensities throughout the series. A unique threshold value could be used to segment the whole 3-D data set. However, the compensation algorithm did not take into account the degradation of the signal-to-noise ratio as a function of depth. Thus, although the average intensities were equalized, the noise level was amplified in the deep sections of the series. The consequence of this amplification is that the segmented nuclei at the top of the series were smoother in shape than the segmented nuclei at the bottom of the series. If we consider the number of voxels that defined the surface of a nucleus (from 1000 to 2500 voxels), and the mathematical principle of the ellipsoid fitting we may assume that the influence of noise would slightly modify the relative sizes of the ellipsoid radii while the major orientation of the ellipsoid would be unchanged. To improve the resolution of individual nuclei a 3-D morphological opening operator was applied to the data set. In our case we used a cubic filter without the corner voxels (van der Voort *et al.*, 1989). This 3-D kernel mimics a small discrete sphere and creates fewer artefacts than a 3-D cubic window. Other authors have used transformed lattices (tetradecahedral or rhombododecahedral) to improve the isotropy of the morphological operator (Rigaut *et al.*, 1990; Conan *et al.*, 1992). Because their original data sets were sampled on a rectangular lattice, these had to be transformed to another grid by resampling. However, the resampling techniques also introduce artefacts and therefore reduce the benefit of using isotropic morphological operators.

Although the method we used for segmentation was satisfactory it could be improved using a different approach, based on 3-D Voronoi diagrams and a split & merge strategy that takes into account local grey-level statistics and is not dependent on the sampling lattice (Bertin *et al.*, 1992, 1993).

Robustness of the ellipsoid model

Using a tri-axial ellipsoid model for fitting provided a good measurement of the orientations of the nuclei. Indeed, in fetal human heart a morphological study of the myocardial cell nuclei showed that in longitudinal sections 80% of nuclei had an oval shape, while 20% were rectangular with rounded corners (Adler *et al.*, 1977). We performed simulation tests in order to assess the accuracy of the orientation measurements for such shapes. In these tests we generated 2-D discrete ellipses and rectangles with varying long axis versus short axis ratios (from 3:1 for ovals to nearly spherical) and varying orientations, their long axes ranging from 0 to 90° by steps of 1°. The results showed that for ellipses the measurement error is balanced symmetrically and did not exceed ±3° in the worst case (nearly-spherical shape). In the case of the rectangles there was a systematic over-estimation of the angle because the method tended to detect the diagonal of the rectangle rather than its longer side. However, in all cases the maximum error never exceeded 3°.

Contaminating interstitial cell nuclei and red blood cells

Interstitial cell nuclei and red blood cells are possible sources of error in the measurement of the main orientation of myocardial cell nuclei. At the fetal stage, the red blood cells have no nucleus but the haemoglobin contained by these cells emits an intense red fluorescence when excited by a 543-nm light source. In order to eliminate as many blood cells as possible the hearts were rinsed thoroughly prior to fixation. Red blood cells have a very typical shape, they are small in volume and they can be described as concave discoids. Therefore, they can be easily discriminated using size and shape criteria (ratio of the ellipsoid radii) from myocardial cells and eliminated from the analysis. Qualitative data about the ratio between myocardial cells and interstitial cells in fetal human hearts can be found in Anderson & Becker (1987) and in Zak (1984). At this stage the interstitial cells represent only a small fraction of the total cells in fetal heart. Unfortunately, to the best of our knowledge no quantitative data have been published for human fetal hearts. The only quantitative data available was established by Cluzeaut & Maurer-Schutze (1986) for the developing mouse. In their study they showed that the ratio of myocardic cells to interstitial cells was 8 during the prenatal stage, then dropped to 1·5 after birth and to 1 21 days after birth. Therefore, the proportion of interstitial cells may be assumed to be close to 10% in fetal human hearts and this level of error in the measurements does not really modify the results for myocardial cells.

Sampling

The analysed zones were very small compared with either the size or the thickness of the sections. In order to obtain more representative information it is necessary to analyse contiguous 3-D blocks. This is possible, although the main limiting factor is the time necessary for the analysis of a single block (1 h 30 min). The other difficulty is the limitation of the working distance of objectives with a high numerical aperture. The working distance of the 40×

objective (NA 1·3) we are using is 120 μm. Actually, only one-fifth of the thickness of the sections could be investigated.

Assessment of anisotropy

Two different models were used to analyse the directional distribution of the nuclei of myocardial cells. Firstly, we used a vectorial analysis such as that described by Batschelet (1981). The main orientation was derived from the vectorial sum of the major directions of the nuclei and a homogeneity factor was calculated. Secondly, we used a statistical approach based on the diagonalization of the matrix of the direction cosines recommended by Anderson & Stephens (1972). In this method the relative amplitudes of latent roots are indicators of the anisotropy. For example, if the values $\tau 1$, $\tau 2$ and $\tau 3$ are very similar, the data set is drawn from an isotropic process. If $\tau 3$ is greater than $\tau 2$ and $\tau 1$ then the directions are clustered around a single axis. For the septum region the two methods provided different results. The vectorial analysis revealed a heterogeneity in the orientations while the other method indicated high anisotropy. This might initially appear contradictory. However, a close examination of the polar diagrams (Fig. 3) explained this ambiguity: the distribution of the azimuth angle appreared bimodal with two modes nearly opposed, one centred on $-90°$ (pointing south) and the other centred on 50° (pointing north-east). Thus, the vectorial sum gave a resultant vector of $-48°$ with a low homogeneity. This translated the opposition of these two populations of fibres. However, when considered separately, these populations were very homogeneous and might be considered as clustered around a single axis orientated along a south to north, north-east direction. This is why the anisotropy measurement by the method of the latent roots was high. In conclusion, the two measurement methods were neither contradictory nor redundant and brought complementary information.

Conclusion

Until now, the existing methods developed for the quantification of myofibre patterns were limited to planar information. For example, McLean & Prothero (1987) developed a semi-automatic approach in which only in-plane myofibres were recorded with a digitizer tablet. Thus, only information about the azimuth angle was accessible. Another approach based on polarized light microscopy was proposed by Whittaker *et al.* (1989). This semi-quantitative analysis deduced the azimuth angle from the transmitted light intensity. However, this study did not take into account the modulation of light intensity due to the elevation angle of the myofibres.

In conclusion, we have developed a series of 3-D image analysis tools for measuring the 3-D orientation of myocardial cell nuclei. The method, based on CSLM, makes it possible to characterize the azimuth angle of nuclei as well as their elevation angle. In the normal fetal heart, because of the existing correlation between nuclei orientations and the orientation of the myocardial cells we may extrapolate the measures from the nuclei to myocardial cells. Unfortunately, it is still a time-consuming method and could not be used as it is for routine study. However, it is a fine and accurate way of assessing and calibrating the information given by polarized light microscopy. Polarized light analysis could be used as a fast and efficient quantitative measurement tool for the 3-D organization of myocardial fibres.

Acknowledgments

This work was supported by the Association Française contre les Myopathies (AFM-90,91,92). The authors wish to thank Dr Victoria Von Hagen for her advice in editing the manuscript, Mr Gandini (Ecole Française de Papeterie et Arts Graphiques) for his expert advice about the chemistry and Mr Cividino for his technical help.

References

Adler, C.P., Hartz, A. & Sandritter, W. (1977) Form and structure of cell nuclei in growing and hypertrophied human hearts. *Beitr. Path.* **161**, 342–362.

Anderson, R.H. & Becker, A.E. (1987) *Cardiac Anatomy*, pp. 92–95. Churchill & Livingston.

Anderson, T.W. & Stephens, M.A. (1972) Tests for randomness of directions against equatorial and bimodal alternatives. *Biometrika*, **59**, 613–621.

Batschelet, E. (1981) *Circular Statistics in Biology*, pp. 214–219. Academic Press, London.

Bertin, E., Marcelpoil, R. & Chassery, J-M. (1992) Morphological algorithms based on Voronoi and Delaunay graphs: microscopic and medical applications. *Image Algebra and Morphological Image Processing III*, pp. 356–357. SPIE San Diego.

Bertin, E., Parazza, F. & Chassery, J-M. (1993) Segmentation and measurement based on 3D Voronoi diagram: application to confocal microscopy. *Computerized Medical Imaging and Graphics*, **17**, 175–182.

Carlsson, K. & Aslund N. (1987) Confocal imaging for 3D digital microscopy. *Applied Optics*, **26**, 3232–3238.

Clarke, A., Davidson, N. & Archenhold, G. (1993) Measurements of fibre direction in reinforced polymer composites. *J. Microsc.* **171**, 69–79.

Cluzeaut, F. & Maurer-Schutze B. (1986) Proliferation of cardiomyocites and interstitial cells in the cardiac muscle of the mouse during pre- and post-natal development. *Cell Tissue Kinetics*, **19**, 267–274.

Conan, V., Gesbert, S., Howard, C.V., Jeulin, D., Meyer, F. & Renard, D. (1992) Geostatistical and morphological methods applied to three-dimensional microscopy. *J. Microsc.* **166**, 169–184.

Duxson, M.J., Usson, Y. & Harris, A.J. (1989) The origin of secondary myotubes in mammalian skeletal muscles: ultrastructural studies. *Development*, **7**, 743–750.

Harris, A.J., Duxson, M.J., Fitzsimons, R.B. & Rieger, F. (1989) Myonuclear birthdates distinguist the origins of primary and secondary myotubes in embryonic mammalian skeletal muscles. *Development*, **107**, 771–784.

Hort, W. (1960) Makroskopische und mikrometrische untersuchungen am myokard verschieden stark gefüllter linker kammern. *Virchows Arch. Pathol. Anat.* **33**, 523–564.

Humbert, C., Santisteban, M.S., Usson, Y. & Robert-Nicoud M. (1992) Intranuclear co-location of newly replicated DNA and PCNA by simultaneous immunofluorescent labelling and confocal microscopy in MCF-7 cells. *J. Cell Sci.* **103**, 97–103.

Jouk, P.S., Usson, Y., Michalowicz, G. & Parazza, F. (1994) Methods for the mapping of the orientation of myocardial cells by means of polarized light. *Microsc. Res. Tech.* (in press).

Kett, P., Geiger, B., Ehemann, V. & Komitowski, D. (1992) Three-dimensional analysis of cell nucleus structures vizualized by confocal scanning laser microscopy. *J. Microsc.* **167**, 169–179.

McLean, M.R. & Prothero, J. (1987) Coordinated three-dimensional reconstruction from serial sections at macroscopic and microscopic levels of resolution: the human heart. *Anat. Record*, **219**, 434–439.

McLean, M.R. & Prothero, J. (1991) Three-dimensional reconstruction from serial sections. V. Calibration of dimensional changes incurred during tissue preparation and data processing. *Anal. Quant. Cytol. Histol.* **13**, 269–277.

Manasek, F.J. (1970) Histogenesis of the embryonic myocardium. *Am. J. Cardiol.* **25**, 149–168.

Maron, B.J. & Roberts, W.C. (1979) Quantitative analysis of cardiac muscle cell disorganization in the ventricular septum of patients with hypertrophic cardiomyopathy. *Circulation*, **59**, 689–706.

Mattfeldt, T., Clarke, A. & Archenhold, G. (1994) Estimation of the directional distribution of spatial fibre processes using stereology and confocal scanning laser microscopy. *J. Microsc.* **173**, 87–101.

Newman, W.M. & Sproull, R.F. (1981) *Principle of Interactive Computer Graphics*, 2nd edition, International Student Edition, pp. 389–410. McGraw-Hill.

Parazza, F., Humbert, C. & Usson, Y. (1993) Method for 3-D volumetric analysis of intranuclear fluorescence distribution in confocal microscopy. *Computerized Medical Imaging and Graphics*, **17**, 189–200.

Rigaut, J-P. & Vassy, J. (1991) High-resolution three-dimensional images from confocal scanning laser microscopy—Quantitative study and mathematical correction of the effects from bleaching and fluorescence attenuation in depth. *Anal. Quant. Cytol. Histol.* **13**, 223–232.

Rigaut, J-P., Vassey, J., Herlin, P., Duigou, F., Masson, E., Mandard, A.M., Calard, P. & Foucrier, J. (1990) DNA cytometry by confocal scanning laser microscopy in thick tissue blocks-methodology and preliminary results in histopathology. *Trans. Roy. Microsc. Soc.*, Vol 1 (ed. by H.Y. Elder), pp. 385–388. Adam Hilger, Bristol.

Streeter, D.D. (1979) Gross morphology and geometry of the heart. *Handbook of Physiology Section 2*, Vol. 1, pp. 61–112.

Streeter, D.D. & Hanna, W.T. (1973) Engineering mechanics for successive states in canine left ventricular myocardium. II. Fibre angle and sarcomere length. *Circulation Res.* **33**, 656–664.

Torrent-Guasp, F. (1973) *The Cardiac Muscle*. Fundaciòn Juan March, Madrid.

van der Voort, H.T.M., Brakenhoff, G.J. & Baarslag, M.W. (1989) Three-dimensional visualization methods for confocal microscopy. *J. Microsc.* **153**, 123–132.

Whittaker, P., Romano, T., Silver, M.D. & Boughner, D.R. (1989) An improved method for detecting and quantifying cardiac muscle disarray in hypertrophic cardiomyopathy. *Am. Heart J.* **118**, 341–346.

Zak, R. (1984) *Growth of the Heart in Health and Disease*. Raven Press, New York.

Appendix

Let S, the set of the surface voxels of a nucleus N, be defined as follows:

$$S\{(x,y,z) \in N / \exists (x+i, y+j, z+k) \notin N; i,j,k \in \{-1,1\}\}. \quad (1)$$

S can also be defined as a matrix with three columns corresponding to the x, y and z coordinates and m rows where m is the number of surface voxels.

Let c_x, c_y and c_z, the coordinates of the centre of gravity of S, be calculated as follows:

$$c_x = \frac{1}{m}\sum_{i=1}^{m} x_i; c_y = \frac{1}{m}\sum_{i=1}^{m} y_i \text{ and } c_z = \frac{1}{m}\sum_{i=1}^{m} z_i \quad (2)$$

where x_i, y_i and z_i are the coordinates of the ith voxel of S.

Let S_c be the matrix of the surface voxels after translation of the origin of the space to the centre of gravity of S such that

$$S_c\{(x-c_x, y-c_y, z-c_z)/(x,y,z) \in S\}. \quad (3)$$

The spatial distribution of the surface voxels is given by the matrix V of the inner products of the columns vectors of the matrix S_c:

$$V = S_c^t S_c \quad (4)$$

where the t superscript denotes matrix transposition.

The orientation of the scatter ellipsoid is obtained by diagonalization of the matrix V, i.e. by solving the linear equation

$$(V - \lambda_i I)\mathrm{U}_i = 0 \quad (5)$$

where I is the identity matrix, λ_i are the latent roots or eigenvalues of the matrix V such that $\lambda_1 \geqslant \lambda_2 \geqslant \lambda_3$ and U_i are the associated eigenvectors. In other words, the radii of the scatter ellipsoid are given by $\sqrt{\lambda_i}$. The rotation of the ellipsoid is defined by the transformation matrix t whose

columns are the eigenvectors

$$\mathbf{U}_i \begin{bmatrix} u_i \\ v_i \\ w_i \end{bmatrix}.$$

Therefore, the normalized orientation vector **D** of a nucleus is given by

$$\mathbf{D} = \begin{bmatrix} \alpha \\ \beta \\ \gamma \end{bmatrix} = t\mathbf{X} = [\mathbf{U}_1\mathbf{U}_2\mathbf{U}_3] \begin{bmatrix} 1 \\ 0 \\ 0 \end{bmatrix}$$
$$= \begin{bmatrix} u_1 & u_2 & u_3 \\ v_1 & v_2 & v_3 \\ w_1 & w_2 & w_3 \end{bmatrix} \begin{bmatrix} 1 \\ 0 \\ 0 \end{bmatrix} = \begin{bmatrix} u_1 \\ v_2 \\ w_1 \end{bmatrix} \tag{6}$$

where **X** is the unit vector along the x-axis. **D** can be represented as a function of two angular components ϕ and θ such that

$$\mathbf{D} = \begin{bmatrix} \alpha \\ \beta \\ \gamma \end{bmatrix} = \begin{bmatrix} \cos\phi\cos\theta \\ \sin\phi\cos\theta \\ \sin\theta \end{bmatrix}. \tag{7}$$

Therefore, the mean azimuth angle ϕ and the mean elevation angle θ for n nuclei are

$$\phi = \begin{cases} \arctan\left(\dfrac{r_y}{r_x}\right) & \text{if } r_x > 0 \\ \Pi + \arctan\left(\dfrac{r_y}{r_x}\right) & \text{if } r_x < 0 \end{cases} \qquad \theta = \arctan\left(\frac{r_z}{\sqrt{r_x^2 + r_y^2}}\right) \tag{8}$$

where rx, ry and rz are given by

$$r_x = \sum_{i=1}^{n} \alpha_i \qquad r_y = \sum_{i=1}^{n} \beta_i \qquad r_z = \sum_{i=1}^{n} \gamma_i.$$

The homogeneity of orientations is given by

$$H = \frac{1}{n}\sqrt{\left(\sum_{i=1}^{n}\alpha_i\right)^2 + \left(\sum_{i=1}^{n}\beta_i\right)^2 + \left(\sum_{i=1}^{n}\gamma_i\right)^2}. \tag{9}$$

The measurement of anisotropy can also be characterized using the latent roots $\tau 1$, $\tau 2$ and $\tau 3$ of the matrix of the direction cosines T:

$$T = \frac{1}{n}\begin{pmatrix} \sum\alpha_i^2 & \sum\alpha_i\beta_i & \sum\alpha_i\gamma_i \\ \sum\beta_i\alpha_i & \sum\beta_i^2 & \sum\beta_i\gamma_i \\ \sum\gamma_i\alpha_i & \sum\gamma_i\beta_i & \sum\gamma_i^2 \end{pmatrix}. \tag{10}$$